

Acetone Complexes for High-Performance Perovskite Photovoltaics with Reduced Nonradiative Recombination

Zhen Wang¹, Chenguang Yang^{1,2}, Yuying Cui², Li Xie¹, Feng Hao^{2,*}

¹Faculty of Printing, Packaging and Digital Media Technology, Xi'an University of
Technology, Xi'an, 710054, China

²School of Materials and Energy, University of Electronic Science and Technology of China,
Chengdu 611731, China

*Corresponding author. E-mail: haofeng@uestc.edu.cn (F. Hao)

Experimental

Materials: Methylammonium iodide (MAI, Great-Cell, 99.9%), lead(ii) iodide (PbI_2 , Aladdin, 99.9%), [6,6]-phenyl-C₆₁-butyric acid methyl ester (PC₆₁BM, Luminescence Technology, 99%), silver (Ag, Trillion Metals, 99.9%), ethanol (General-Reagent, 99.7%), acetone (Cdkelong, 99.5%), isopropanol (IPA, Aladdin, 99.8%), ethylene glycol (Cdkelong, 99.5%), ethylenediamine (Cdkelong, 99.0%), N-methyl-2-pyrrolidone (NMP, General-Reagent, 99.0%), N,N-dimethylformamide (DMF, Sigma-Aldrich, 99.8%), diethyl ether (DE, KESHI, 99.5%), chlorobenzene (CB, Sigma-Aldrich, 99.8%), nickel acetate tetrahydrate (Adamas-beta, 98%), and polyethyleneimine (PEI, Sigma-Aldrich, 50% (w/v) in H₂O) were used as received without further purification.

Device preparation: Fluorine-doped tin oxide (FTO) conducting glass was ultrasonically cleaned with detergent, deionized water, ethanol, acetone, and isopropanol successively. Then, the substrate was dried with a stream of nitrogen and treated with UV-ozone for 15 minutes. 0.5 M nickel acetate tetrahydrate in ethylene glycol and equivalent ethylenediamine was spin-coated on the substrate at 4000 rpm in ambient temperature. The NiO_x layer was annealed in a muffle furnace at 350 °C for an hour. The precursor solution of the perovskite absorber layer was prepared by dissolving PbI_2 and MAI (1.35 M) in mixture solvent. The mixture solvent was prepared by mixing acetone and a solvent mixture of NMP: DMF=9: 8 (v: v) at volume ratios of 0: 300, 30: 270, 40: 260, 50: 250, 60: 240. The perovskite precursor solution was spin-coated on NiO_x layer at 3000 rpm for 70 s with 1 mL diethyl ether dripping at the last 25 s, and then annealed at 100 °C for 10 min. A layer of PC₆₁BM (20 mg mL⁻¹ in CB) was spin-coated at 3000 rpm for 30 s. After that, a PEI solution (dissolved in IPA) was spin-coated onto the layer of PC₆₁BM at 4000 rpm for 30 s. Finally, 100 nm Ag electrode was thermally evaporated on the top of PEI layer under high vacuum conditions. The entire formation process of the cell device was completed in a N₂ atmosphere glove box, except for the NiO_x layer.

Device characterization: X-ray diffraction (XRD) spectrum was obtained by a MiniFlex 600 (Rigaku) X-ray diffractometer with Cu Ka radiation ($\lambda = 0.15406$ nm, 40 kV, 100 mA). The *J-V* characteristics of the solar cell devices were measured using

a Keithley 2400 source and the solar simulator (San-EI Electric) with standard AM 1.5G (100 mW cm^{-2}) illumination under ambient conditions. The micrograph of perovskite film was measured using high-resolution scanning electron microscopy (Gemini SEM 300). The UV-vis spectra of the perovskite film was measured using UV-2600 spectroscopy (Shimadzu) with an integrating sphere. The steady photoluminescence (PL) spectra was obtained by a Flou Time 300 (PicoQuant). A QE-R (Enlitech) was used to measure the monochromatic incident photon to current conversion efficiency (IPCE). A Paios 2.0 system (FLUXiM) was used to measure transient photocurrent decays (TPC), transient photovoltage decays (TPV) and impedance spectroscopy (IS) data.

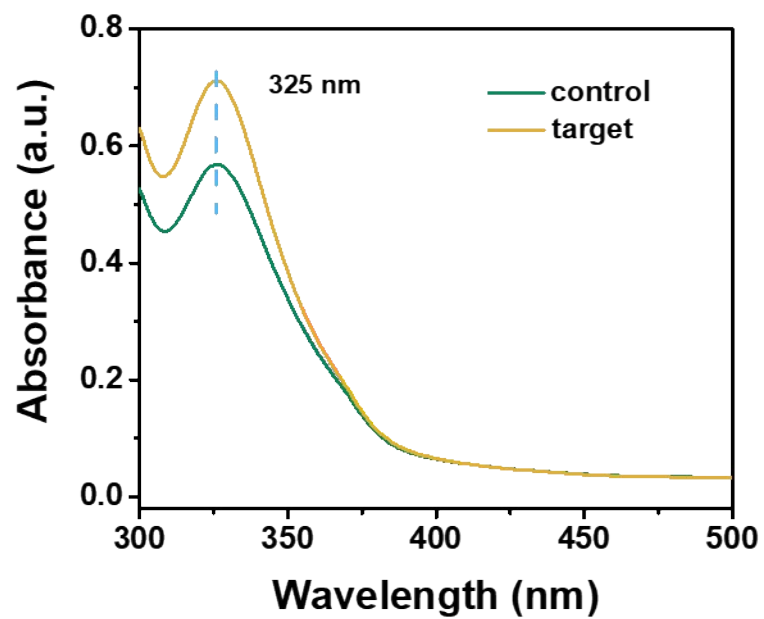


Fig. S1 UV-vis absorbance spectra of control and target precursor solution in mixture solvent (NMP:DMF=9:8)

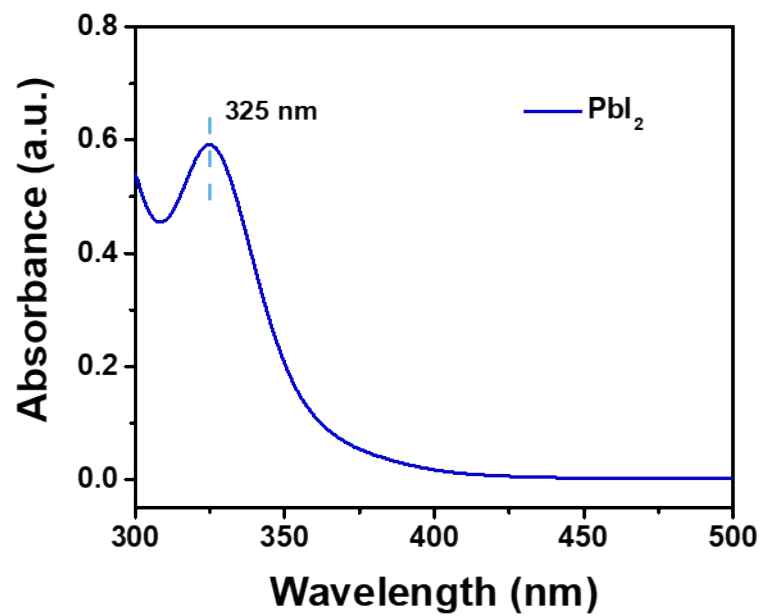


Fig. S2 UV-vis absorbance spectra of PbI_2 dissolved in mixture solvent (NMP:DMF=9:8)

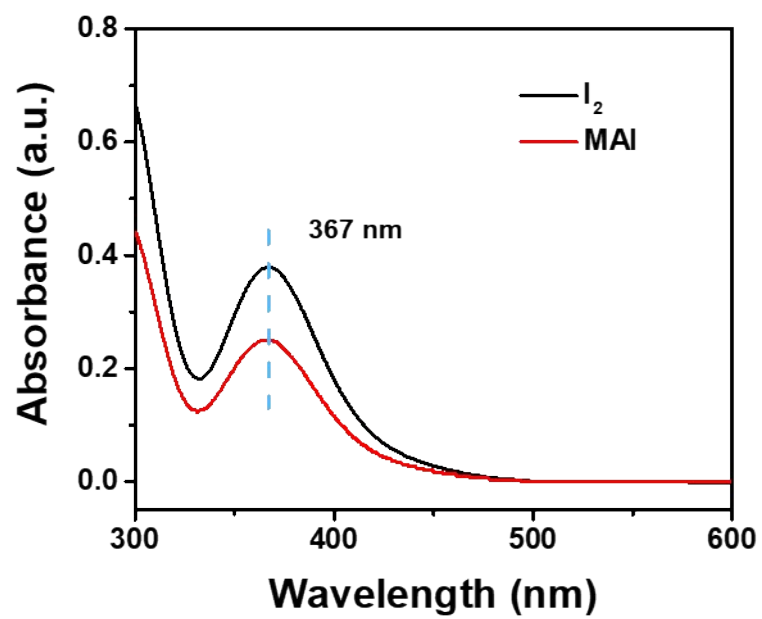


Fig. S3 UV-vis absorbance spectra of I₂ and MAI dissolved in mixture solvent (NMP:DMF=9:8)

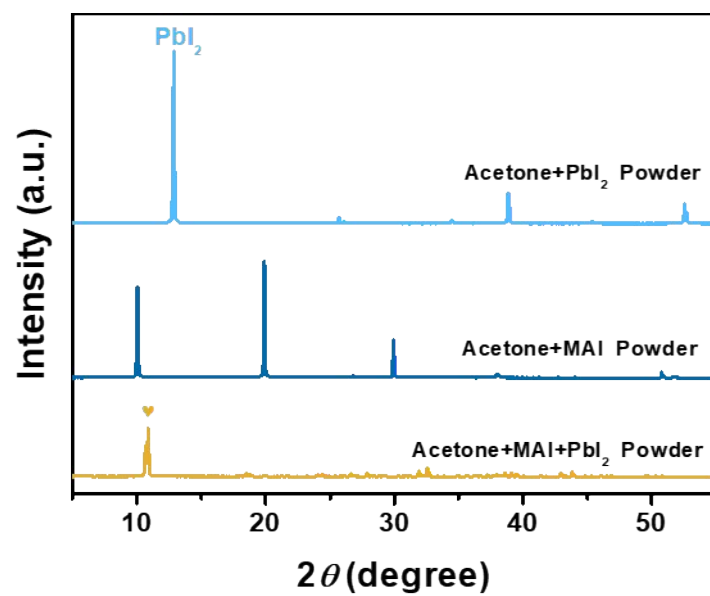


Fig. S4 XRD spectra of Acetone+MAI+PbI₂ complex powder, Acetone+PbI₂ powder, and Acetone+MAI powder.

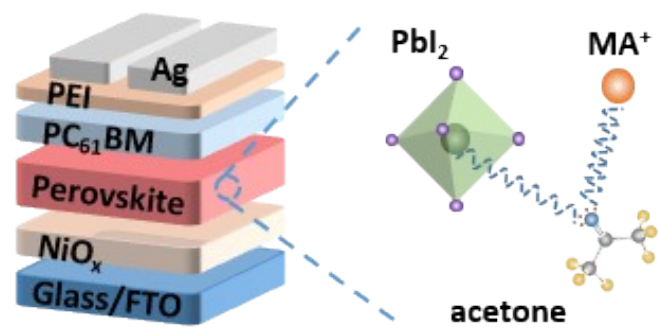


Fig. S5 Schematic diagram of acetone-MAI-PbI₂ complex structure.

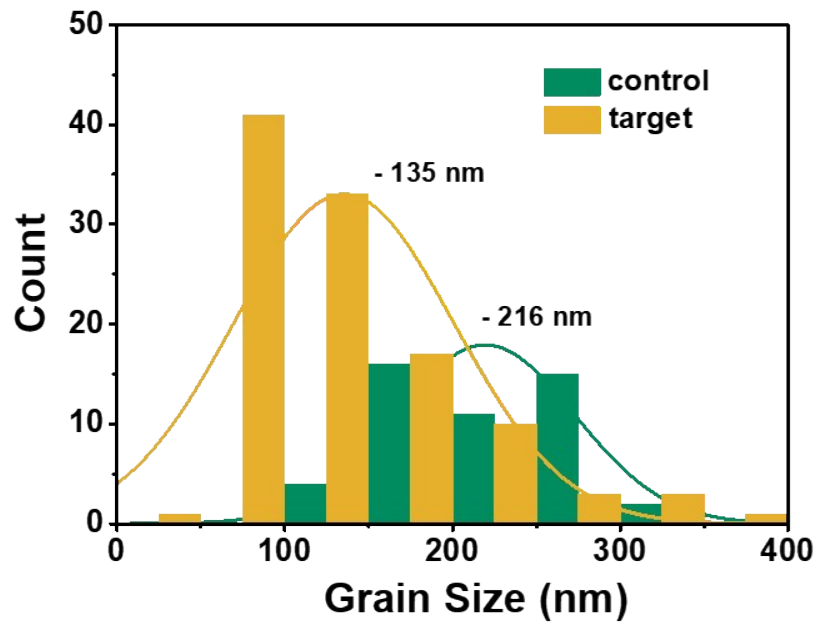


Fig. S6 The histograms of the grain size distribution for the control and target films with the average grain size marked.

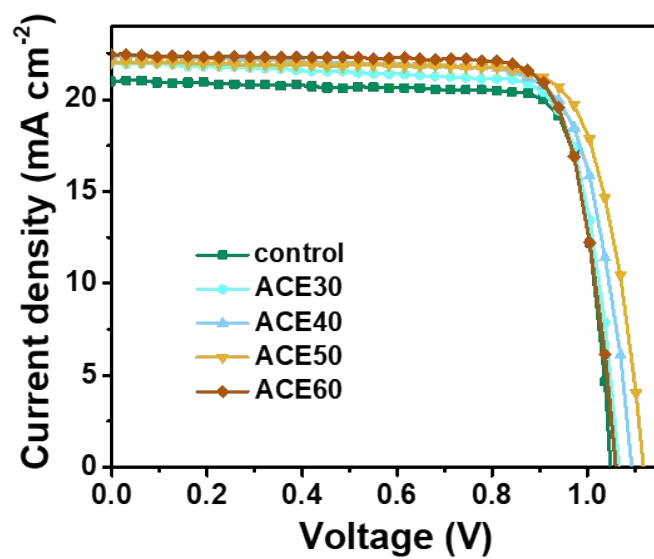


Fig. S7 Photocurrent-voltage ($J-V$) curves for PSC devices with different volume ratios of acetone.

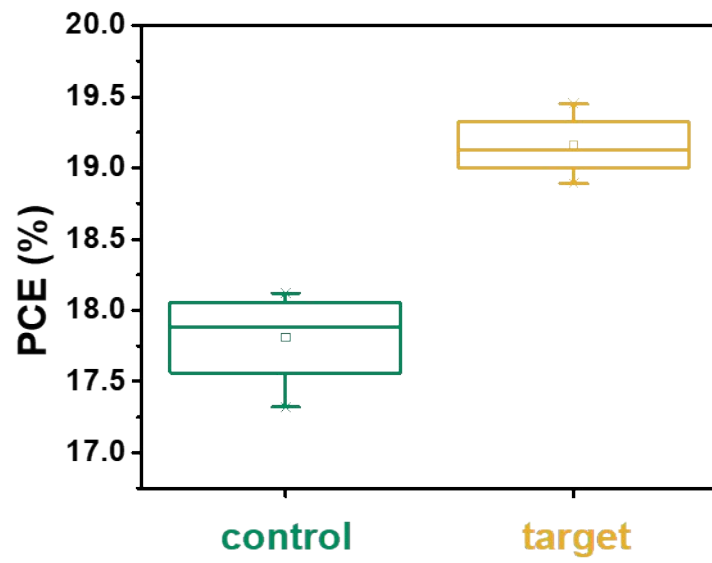


Fig. S8 Statistical distribution of PCE for a batch of 25 independent devices.

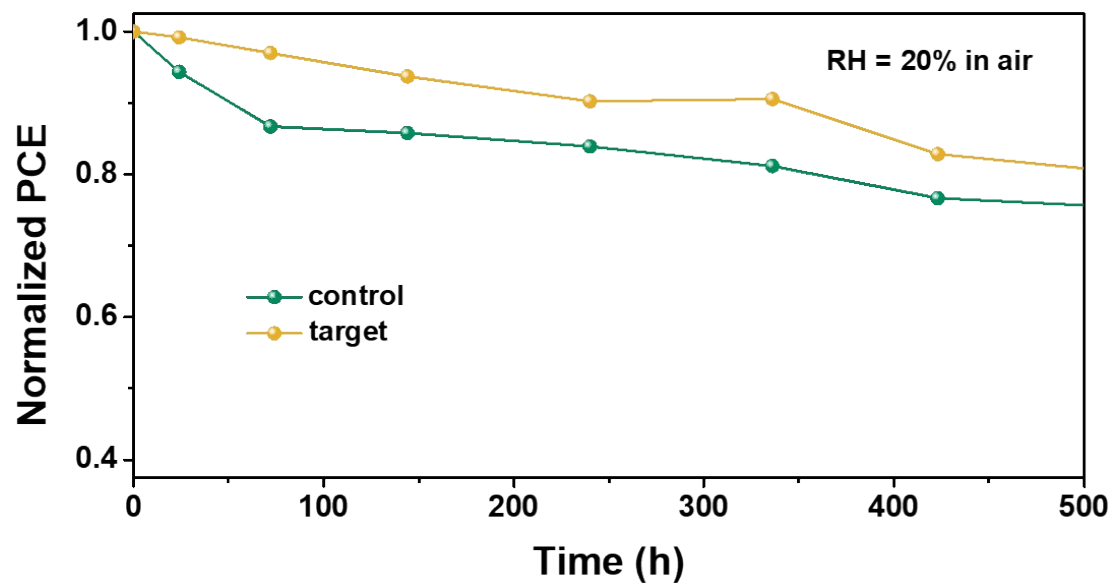


Fig. S9 The normalized PCE decays for the control and target device under 20% RH.

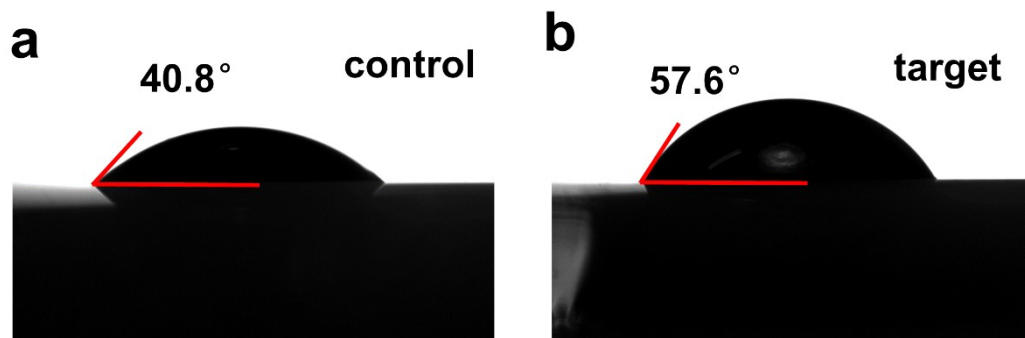


Fig. S10 The water contact angles for the (a) control film and (b) target film.

Table S1 The environmental and healthy impact factor of different solvents.¹ (The higher the score, the greener it is.)

Solvent	Environmental impact	Healthy impact
acetone	9	8
DMF	6	2
NMP	6	3
DMSO	5	7

Table S2 Detailed photovoltaic performance of PSCs with different Ratios of Acetone.

	J_{sc} (mA cm ⁻²)	V_{oc} (V)	FF (%)	PCE (%)
control	21.04	1.05	82.14	18.12
ACE30	21.97	1.07	79.20	18.53
ACE40	22.37	1.09	77.02	18.84
ACE50	22.01	1.12	79.02	19.45
ACE60	22.43	1.06	79.78	18.98

Table S3 Parameters of the EIS analysis of the control and target PSCs.

	R_s (Ω)	R_{rec} (Ω)	C (nF)
control	8.94	310	6.87
target	5.25	575	3.18

Table S4 Parameters of the photo-CELIV analysis of the control and target PSCs.

	A (V/s)	t_{max} (μ s)	j_0 (mA cm ⁻²)	Δj (mA cm ⁻²)	μ (cm ² V ⁻¹ s ⁻¹)
control	1.007×10^5	3.126	1.049	3.491	9.22×10^{-4}
target	1.007×10^5	2.250	1.049	4.524	1.49×10^{-3}

References

1. R. K. Henderson, C. Jiménez-González, D. J. C. Constable, S. R. Alston, G. G. A. Inglis, G. Fisher, J. Sherwood, S. P. Binks and A. D. Curzons, *Green Chem.*, 2011, 13, 854-862.